~~SECRET~~

NACA

RESEARCH MEMORANDUM

DESIGN AND PERFORMANCE OF FLIGHT-TYPE LIQUID-HYDROGEN HEAT EXCHANGER

By David B. Fenn, Willis M. Braithwaite,
and Paul M. Ordin

Lewis Flight Propulsion Laboratory
Cleveland, Ohio

NATIONAL ADVISORY COMMITTEE
FOR AERONAUTICS

WASHINGTON
August 19, 1957

NACA RM E57F14

NATIONAL ADVISORY COMMITTEE FOR AERONAUTICS

RESEARCH MEMORANDUM

DESIGN AND PERFORMANCE OF FLIGHT-TYPE LIQUID-HYDROGEN HEAT EXCHANGER

By David B. Fenn, Willis M. Braithwaite
and Paul M. Ordin

SUMMARY

A liquid-hydrogen fuel system was developed to operate one of the turbojet engines in a twin-engine light bomber at an altitude of 50,000 feet and a flight Mach number of 0.75. A ram-air heat exchanger was used in this fuel system to vaporize the liquid hydrogen.

The heat exchanger was evaluated in an altitude test chamber at the NACA Lewis laboratory in conjunction with the complete aircraft fuel system. The experimental results presented in this report indicate that a ram airflow of 1.76 pounds per second was sufficient to vaporize 565 pounds per hour of fuel. At this condition the air-side temperature drop was 62° R, the average tube wall temperature was 346° R, and the heat-transfer coefficient between the tube wall and the fuel was about 69 Btu/(hr)(sq ft)(°R).

Some fuel system instabilities were encountered during the investigation. Although these could be of a very serious nature, in this case they did not hamper flight operations.

INTRODUCTION

The problems involved in the use of high-energy fuels for obtaining increased range and altitude capabilities for military aircraft are currently under study. Liquid hydrogen is one such fuel which is attractive because of its high heat of combustion and its potentialities as a heat sink for cooling. The structural problems imposed by the high temperatures associated with high flight speeds will present major difficulties unless many aircraft and engine components are cooled. An analysis of the advantages of hydrogen as a coolant and the potential increases in aircraft range and altitude are presented in reference 1. The medium used for cooling the aircraft structure, turbine, afterburner liner, and aircraft component parts may include ram air, compressor bleed air, or exhaust gas which has been cooled in passage through a heat exchanger designed to vaporize and superheat liquid hydrogen.

A project was established at the NACA Lewis laboratory to study the problems associated with the use of hydrogen in aircraft by developing and flight testing a complete hydrogen fuel system. The project involved the modification of an existing twin-engine light bomber to include the hydrogen fuel system. The fuel system was designed to operate one of the two turbojet engines in the aircraft for 1/2 hour at an altitude of 50,000 feet at a flight Mach number of 0.75. Liquid hydrogen was stored in a wingtip fuel tank, vaporized in a ram-air heat exchanger, and burned in the turbojet engine which was modified for use with either JP-4 or hydrogen fuel. Since the heat-sink potential of the fuel was not utilized in this initial aircraft fuel system, the heat exchanger was designed merely to vaporize the fuel in order to provide a uniform fluid for control purposes.

The complete hydrogen fuel system was operated in conjunction with the turbojet engine in an altitude test chamber prior to flight testing. This report presents a description of the ram-air heat exchanger and summarizes the heat-exchanger performance data obtained during the altitude test chamber investigation. In addition, a discussion of the instrumentation used for low-temperature measurements is included.

AIRCRAFT FUEL SYSTEM

The fuel system used for this investigation and the aircraft flight tests (fig. 1) was designed to operate one engine with hydrogen for approximately 1/2 hour at an altitude of 50,000 feet and a flight Mach number of 0.75. Hydrogen was stored as a liquid in the wingtip tank which was insulated with a polystyrene foam plastic. A complete description of the fuel tank is included in reference 2. A helium gas pressurizing system was used to force the fuel through the system to the combustor. Vacuum-insulated piping was used between the tank and the heat exchanger to prevent vaporization in the liquid flow line. The cold hydrogen gas was conducted from the heat exchanger through a hydrogen flow regulator to the turbojet combustor. A description of the regulator and the combustor together with their performance is contained in references 3 and 4.

The heat exchanger was included in this fuel system to provide a uniform fluid as a vapor to simplify fuel flow control. This heat exchanger was designed to vaporize the 520 lb/hr of hydrogen required by the engine at the selected flight condition. In order to minimize engine modifications, ram air was chosen for the heat source instead of compressor bleed air or exhaust gas. Since the cooling potential of the fuel was not utilized in this initial aircraft fuel system, the entire difference between total and static pressures associated with the flight condition was available to force air through the heat-exchanger core and associated ducting. To prevent the formation of liquid or solid air on the heat-exchanger tubes, the unit was sized to maintain wall temperatures well above the boiling point of air (approx. 140° R).

The requirements of the heat exchanger which were specified by the selected flight and engine operating conditions at 50,000 feet are summarized as follows:

Inlet air total temperature, °R	437
Inlet air total pressure, lb/sq ft abs	353
Altitude static pressure, lb/sq ft abs	243
Fuel flow, lb/hr	520
Fuel pressure, lb/sq in. abs	55
Inlet fuel temperature, °R (saturated liquid)	46
Tube wall temperature, °R	>140

APPARATUS

Heat Exchanger

A schematic diagram of the heat exchanger used in this investigation and for the aircraft flight tests is presented in figure 2. The heat-exchanger core was constructed in a simple crossflow arrangement using short finned tubes manifolded together at the top and bottom to provide vertical flow of the fuel inside the tubes. This configuration was used in an effort to avoid the severe unsteady flow conditions reported in references 5 and 6. The unit reported in reference 5 was constructed by using a multipass arrangement of finned tubes which resulted in long narrow fuel passages. It was believed that the flow instabilities were a result of the long narrow fuel passages in the heat exchanger. In the present investigation liquid hydrogen entered the bottom manifold and was vaporized inside the tubes by the ram air flowing over the external fins. Hydrogen gas was collected in the upper manifold where splash plates were installed to minimize liquid carryover. The inlet and outlet manifolds were of welded stainless-steel construction silver-soldered to the copper tubes. Integral finned copper tubes were selected for this core to ensure good thermal contact between the fins and the tubes. A photograph of the inlet air side of the heat exchanger is presented in figure 3, and the dimensions of the tubes and the core are summarized as follows:

Integral finned copper tubes

Length, in.	12
Inside diameter, in.	5/8
Wall thickness, in.	0.049
Fin spacing, fins/in.	7
Fin outside diameter, in.	$1\frac{1}{2}$
Mean fin thickness, in.	0.024

[redacted]

Core

Total number of tubes	28
Width (normal to fuel and air flows), in.	$9\frac{3}{4}$
Height (parallel to fuel flow), in.	12
Length (parallel to airflow), L, in.	7
Frontal area, sq ft	0.813
Ratio of free flow area on air side to frontal area	0.475
Air-side heat-transfer area, sq ft	45.9
Fuel-side heat-transfer area, sq ft	4.6

Altitude Test Chamber

A photograph of the altitude test chamber installation of the hydrogen fuel system including the turbojet engine is presented in figure 4. The component parts of the system are identical to those later installed in the aircraft. The heat-exchanger manifolds were insulated with a plastic foamed in place to simplify the evaluation of heat-exchanger performance by minimizing heat leak to these areas. A bulkhead with a labyrinth seal around the engine inlet was used to allow independent control of the engine-inlet total pressure and the altitude static pressure. Ram air for the heat exchanger was obtained ahead of this bulkhead. The outlet air side of the heat exchanger was open to the engine compartment (altitude static pressure). A butterfly valve in the heat-exchanger inlet duct was provided to adjust the ram airflow.

Instrumentation

The evaluation of heat-exchanger performance is dependent upon the measurement of air, fuel, and tube wall temperatures. Copper-constantan thermocouples referenced to liquid nitrogen, boiling at atmospheric pressure, were used to measure the inlet and outlet air temperatures as well as the tube wall temperatures.

The sensitivity of a thermocouple to temperature changes decreases rapidly as the temperature level is reduced. The variation of signal strength with temperature for a copper-constantan thermocouple is shown in figure 5. For temperatures in the range of liquid hydrogen (40° to 60° R) a signal strength of only 0.005 mv/$^{\circ}$R is obtained. However, if the change in resistance of a carbon resistor is calibrated with temperature for a constant current flow, a signal strength of 0.215 mv/$^{\circ}$R can be obtained in the same temperature range (fig. 5). Therefore, carbon resistors were used to measure the temperature of the fuel at the inlet and outlet of the heat exchanger. The circuitry necessary to use a carbon resistor is shown in figure 6 with the dimensions of the particular probes

used in this investigation. A constant current of 0.1 milliamp was supplied to the resistor with the 6-volt battery, and the recording potentiometer was used to measure the voltage drop across the resistor. The current flow was measured with the 150-ohm precision resistor and adjusted with the variable 5000-ohm resistor. Periodic checks of the current flow were made to ensure consistent results.

The location of the air-side heat-exchanger instrumentation is shown schematically in figure 7. Total-pressure and -temperature surveys were made in the airstream at the inlet and outlet of the core (stations 2 and 3). The ram airflow was measured in the 7-inch-diameter duct ahead of the core (station 1) because the Mach number at this station was considerably higher than at the heat-exchanger inlet. The temperatures of the tube walls were measured with copper-constantan thermocouples peened into the wall at the base of the fins. The lead wires were wrapped once around the tube in the spiral spaces between the fins to minimize conduction errors. Four thermocouples were attached to each of two tubes in the banks of tubes at the air inlet and outlet of the heat exchanger. Their actual locations are shown in the photograph of the inlet air side of the core (fig. 3).

4605

PROCEDURE

The heat exchanger was operated in conjunction with a turbojet engine in an altitude test chamber. To minimize the time required to cool the fuel system to its steady-state operating condition, the heat exchanger was cooled with ram air before starting the flow of hydrogen. In addition, the ram airflow was maintained at a low value after starting until the heat-exchanger-outlet fuel temperature decreased to about 140° R. The ram air was supplied at total temperatures ranging from 430° to 451° R with a moisture content of less than 0.5 grain per pound of dry air. The heat-exchanger-inlet total pressure was varied from 250 to 400 lb/sq ft abs to obtain a range of ram airflows. The range of fuel flows and ram airflows included in this investigation is summarized in the following table:

Airflow, w_a, lb/sec	Fuel flow, w_f, lb/hr
1.76	351 to 505
1.83	151 to 518
2.12	265 to 622
0.361 to 1.87	522
.537 to 2.21	571
.495 to 1.83	613

(All symbols are defined in appendix A.) An attempt was made to calculate fuel flow from measurements made with a venturi located in the gas line between the hydrogen regulator and the engine. However, these results were inconsistent because the exact thermodynamic state of the gas could not be determined at temperatures close to that of the liquid. Erratic changes in the heat-exchanger-outlet temperature indicated that some liquid carryover was taking place. Therefore, the fuel flow rates presented were calculated from the performance of the turbojet engine with an assumed combustion efficiency of 98 percent (ref. 3).

RESULTS AND DISCUSSION

Calculated Heat-Exchanger Performance

The heat exchanger was designed to supply the latent heat of vaporization of 520 lb/hr of liquid hydrogen using ram air as a heat source. The methods of calculation used in the heat-exchanger design are presented in appendix B where the performance of the heat exchanger is calculated for the design conditions. These calculations indicated that an airflow of 1.75 lb/sec would be sufficient to vaporize 520 lb/hr of fuel and that the air-side temperature drop would be 57.8° R. The average tube wall temperature computed for the design condition was 309° R, and the fuel-side film coefficient was 71.5 Btu/(hr)(sq ft)(°R). Because of the high wall temperatures necessary to prevent the formation of liquid air, the heat exchanger was forced to operate in the film boiling region. Reference 7 indicates that hydrogen boils in this region when the temperature difference between the tube wall and the liquid is above 10° R.

For an airflow of 1.75 lb/sec and a fuel flow of 520 lb/hr the total-pressure loss on the air side of the heat exchanger was calculated to be 53 lb/sq ft.

Experimental Heat-Exchanger Performance

The heat-exchanger performance data obtained during this investigation are presented in table I.

Air-side total-pressure loss. - The variation of the air-side total-pressure-loss ratio $(P_2 - P_3)/P_2$ with corrected ram airflow is presented in figure 8 for three fuel flow rates. The ram airflow was corrected to NACA standard sea-level conditions by use of the conventional parameters of temperature ratio θ and pressure ratio δ to account for variations in inlet conditions (ref. 8). The design airflow of 1.75 lb/sec at the 50,000-foot flight condition corresponds to a corrected sea-level airflow of 9.7 lb/sec for which a total-pressure-loss ratio of 0.175 was obtained.

[redacted]

This amounts to a total-pressure loss of 62 lb/sq ft for the design airflow. The effect of fuel flow on the air-side total-pressure-loss ratio could not be detected within the range of fuel flows investigated.

Vaporization capacity. - The ability of the heat exchanger to vaporize fuel can be illustrated by the ratio of the heat lost by the air to the latent heat of vaporization of the fuel flowing through the heat exchanger. Values of this enthalpy ratio equal to 1.0 indicate complete vaporization of the fuel while values greater than 1.0 show a degree of superheating. Enthalpy ratios below 1.0 indicate incomplete vaporization and may be interpreted as fuel quality; that is, a weight ratio of gas flow to total flow. The enthalpy ratio is plotted as a function of ram airflow in figure 9(a) for three fuel flows. With a fuel flow of 522 lb/hr an airflow of 1.4 lb/sec was required for complete vaporization. The maximum fuel flow which could be completely vaporized by this heat exchanger was 565 lb/hr as shown in figure 9 where enthalpy ratio is presented as a function of fuel flow for three airflow rates. The airflows investigated are limited to a range from 1.76 to 2.12 lb/sec and resulted in grouping all the data around a single curve. Fuel flow rates less than 565 lb/hr were superheated by the airflows presented as indicated by values of the enthalpy ratio greater than 1.0.

Fuel temperature rise. - The amount of superheat obtained is shown in figure 10 where fuel temperature rise is presented as a function of fuel flow for three airflows. The apparent scatter of these data was attributed to the erratic nature of the fuel outlet temperature probably caused by a small degree of liquid carryover from the heat exchanger. Because of the scatter only two curves could be drawn, one for airflows of 1.76 and 1.83 lb/sec and one for an airflow of 2.12 lb/sec. For the lower ram airflows the amount of superheat varied from about 30° R at a fuel flow of 300 lb/hr to zero at a fuel flow of 565 lb/hr.

Tube wall temperature. - To prevent the formation of liquid or solid air, the heat exchanger was operated with tube wall temperatures well above the boiling point of air. The average tube wall temperatures for the banks of tubes at the air inlet and outlet of the heat exchanger are presented as functions of fuel and airflows in figure 11. The individual temperature measurements, located as shown in figure 3, were arithmetically averaged for the inlet and outlet banks of tubes. The average tube temperature on the air outlet side increased from about 220° to 340° R as the airflow was increased from 0.4 to 2.2 lb/sec with a fuel flow of 522 lb/hr. The effect of varying fuel flow from 522 to 613 lb/hr was not discernible. The inlet bank of tubes was about 50° R warmer than the outlet bank of tubes. The effect of fuel flow on the average tube wall temperatures (fig. 11) indicates very little change in wall temperature through a wide range of fuel flow for the airflow rates investigated. For example, with an airflow of 2.12 lb/sec the average air inlet wall temperature decreased from 382° to 376° R as fuel flow was increased from

300 to 600 lb/hr. A comparison of both parts of figure 11 shows that the tube wall temperatures were more sensitive to changes in airflow than fuel flow.

Fuel-side heat-transfer coefficient. - The fuel-side heat-transfer coefficient was calculated from an average of all the tube wall temperature measurements and the average enthalpy drop of the air. No attempt was made to refine the calculations to account for heat transfer through the inlet and outlet fuel manifolds. The fuel-side heat-transfer coefficient is presented as a function of fuel flow for three airflow rates in figure 12. The data for the three airflows were grouped around a single curve. Figure 13 shows that the fuel-side heat-transfer coefficient increased from 50 to 70 Btu/(hr)(sq ft)($^{\circ}$F) as fuel flow was increased from 150 to 600 lb/hr for an airflow range from 1.76 to 2.12 lb/sec.

4605

Air temperature rise. - Although the cooling capability of the fuel was not utilized in this investigation, the extent to which air can be cooled by the vaporization of liquid hydrogen is of interest. The average temperature drop of the air is presented in figure 13 as a function of both airflow and fuel flow. The temperature drop of the air varied from about 135° R at an airflow of 0.4 lb/sec to 50° R at an airflow of 2.2 lb/sec for a fuel flow range from 522 to 613 lb/hr. The effect of fuel flow on the temperature drop of the air was not pronounced. For example, with an airflow of 1.83 lb/sec the temperature drop of the air increased from about 40° to 60° R as the fuel flow was increased from 150 to 525 lb/hr. Comparison of figures 13 and 11 shows that the air temperature drop follows the trends observed for the average tube wall temperatures.

Temperature profiles. - Some insight into the variation of the fuel-side heat-transfer coefficient along the length of the tube can be obtained from the air and tube wall temperature profile since any change in coefficient would be reflected in these profiles. Typical wall temperature profiles measured along the inlet and outlet tubes of the heat exchanger are presented in figure 14 for several fuel and air flows. The tube walls are colder near the top and bottom manifolds because of conduction from the warm tubes to the cold manifolds.

Air temperature gradients at the inlet and outlet of the core were measured at the same conditions as the wall temperatures and are presented in figure 15. The inlet air was warmer near the duct walls because the altitude test chamber was warmer than the ram-air supply. The outlet air temperature profile was of the same general shape as the tube wall temperature profile. Since no discontinuities were observed in these temperature profiles and their shapes were unaffected by changes in fuel flow, it is believed that no abrupt change in fuel-side heat-transfer coefficient existed along the length of the tubes. It is further believed that the tube walls were covered by a layer of gas surrounding a core of boiling liquid. The boiling within the tubes was probably very violent. This

broke the liquid into small droplets some of which were probably carried into the upper manifold. As the droplets struck the splash plates in the upper manifold, they may have been collected to some extent and fallen back into the tubes. Some liquid carryover was evidenced by the erratic behavior of the fuel outlet temperature as mentioned previously.

Reliability

The heat exchanger was operated for 23 hours during the development of the aircraft fuel system. During this time 38 runs were made. In each run the heat-exchanger-outlet fuel temperature was forced to decrease from about 500° to 100° R in about 30 seconds. No failure of the welded or silver-soldered joints in the heat exchanger was encountered during the investigation.

The engine was operated stably with as much as 50-percent-unvaporized fuel leaving the heat exchanger. In these cases a fairly uniform mixture of gas and liquid must have been present at the heat-exchanger outlet. This was probably due to the violent type of boiling in the heat-exchanger tubes and the use of splash plates in the upper manifold as mentioned previously.

Some oscillations of fuel flow were encountered during the initial portion of some of the runs and caused variations in engine speed of $\pm 1\frac{1}{2}$ percent (ref. 3). Although not generally acceptable, these instabilities could be tolerated for the flight tests of this initial hydrogen fuel system because their effect on aircraft performance was small and they damped out within 10 minutes of operation. In the investigation reported in reference 5, however, the fuel system was so unstable that an automatic high-response control had to be used to permit engine operation. It is believed that the instabilities in liquid-hydrogen fuel systems originate in the heat exchanger. However, the exact mechanism of these instabilities is not understood. Therefore, further research is required before a completely satisfactory heat exchanger can be designed.

The heat exchanger of this report was examined several times for ice formation immediately after hydrogen operation with ram air still flowing. No ice was found on the tubes. The ram air used for this investigation had a moisture content of less than 0.5 grain per pound of dry air. Ice formation on the heat-exchanger tubes may become important in the design of heat exchangers to operate at lower altitudes where more moisture is present in the air. However, further research is required to determine the quantity of moisture which can be tolerated and the nature of the ice formation.

[redacted]

SUMMARY OF RESULTS

A ram-air heat exchanger was built to vaporize the liquid-hydrogen required by a turbojet engine at an altitude of 50,000 feet and a flight Mach number of 0.75. The heat exchanger was designed to vaporize 520 pounds per hour of liquid hydrogen using 1.75 pounds per second of ram air as a heat source. The predicted performance of the heat exchanger agreed fairly closely with the experimental results.

Experimental results presented in this report indicate that a ram airflow of 1.76 pounds per second was sufficient to vaporize 565 pounds per hour of fuel. At this condition the air-side temperature drop was 62° R. The heat-transfer coefficient between the fuel and the tube wall increased from 50 to 70 Btu/(hr)(sq ft)($^{\circ}$R) as fuel flow was increased from 150 to 600 pounds per hour for an airflow range from 1.76 to 2.12 pounds per second.

Some fuel system instabilities occurred during the initial portion of some of the runs made. It is believed that these instabilities originated in the heat exchanger. However, further research is required to fully understand the mechanism of the instabilities and their relation to other fuel system components. Although previous liquid-hydrogen fuel systems have been very unstable, the instabilities associated with this fuel system were of small enough magnitude and duration to permit flight operations.

Lewis Flight Propulsion Laboratory
National Advisory Committee for Aeronautics
Cleveland, Ohio, June 14, 1957

4605

[redacted]

460b

CM-2 back

APPENDIX A

SYMBOLS

A_a	air-side heat-transfer area, sq ft
A_c	air-side free-flow area, sq ft
A_f	fuel-side heat-transfer area, sq ft
A_{fr}	heat-exchanger frontal area, sq ft
c_p	specific heat, Btu/(lb)(^oR)
E	cooling effectiveness, $\frac{\Delta T_a}{T_{a,2} - T_f}$
f	friction factor
G	weight flow rate per unit area, lb/(hr)(sq ft)
g	acceleration due to gravity, ft/sec^2
H	enthalpy, Btu/lb
H_L	latent heat of vaporization, Btu/lb
h_a	air-side heat-transfer coefficient, Btu/(hr)(sq ft)(^oF)
h_f	fuel-side heat-transfer coefficient, Btu/(hr)(sq ft)(^oF)
L	length of core parallel to airflow, ft
NTU	maximum number of heat-transfer units
P	total pressure, lb/sq ft abs
Pr	Prandtl number
p	static pressure, lb/sq ft abs or lb/sq in. abs
Re	Reynolds number
r_h	hydraulic radius
T	indicated temperature, ^oR

U	over-all heat transfer coefficient, Btu/(hr)(sq ft)(^{o}R)
w	weight flow
δ	ratio of inlet total pressure to NACA standard sea-level pressure
η_o	over-all fin efficiency
θ	ratio of inlet total temperature to NACA standard sea-level temperature
μ	absolute viscosity, lb/(hr)(ft)
ρ	density, lb/cu ft
Ω	electrical resistance, ohms

Subscripts:

a	air
f	fuel
m	mean
w	wall
1	station in inlet air duct for airflow measurement
2	heat-exchanger inlet
3	heat-exchanger outlet

APPENDIX B

DESIGN CALCULATIONS

A summary is presented of the calculations involved in the design of the heat exchanger used to vaporize the liquid hydrogen for the aircraft flight tests. The heat exchanger used for these studies may not represent the optimum design, but the important factors are satisfactory operation under the established flight conditions, safety, and the availability of commercial heat-exchanger-core material. A trial-and-error series of calculations similar to that in reference 9 was carried out in an effort to match the heat-transfer characteristics of the core to its air-side total-pressure loss. The methods of calculation used can best be illustrated by evaluating the resulting core. The following conditions were specified by the selection of the flight and engine operating conditions:

Altitude, ft	50,000
Flight Mach number	0.75
Inlet air total temperature, $^{\circ}R$	437
Inlet air total pressure, lb/sq ft abs	353
Altitude static pressure, lb/sq ft abs	243
Fuel flow, lb/hr	520
Fuel pressure, lb/sq in. abs	55
Inlet fuel temperature, $^{\circ}R$ (saturated liquid)	46
Average tube wall temperature, $^{\circ}R$	>140

The following conditions resulted from the trial-and-error calculations:

Ram airflow, lb/sec	1.75

Integral finned copper tubes

Length, in.	12
Inside diameter, in.	5/8
Wall thickness, in.	0.049
Fin spacing, fins/in.	7
Fin outside diameter, in.	$1\frac{1}{2}$
Mean fin thickness, in.	0.024

Core dimensions (see fig. 2)

Total number of tubes	28
Width (normal to fuel and air flows), in.	$9\frac{3}{4}$
Height (parallel to fuel flow), in.	12
Length (parallel to airflow), in.	7

[redacted]

The following areas are necessary to evaluate the performance of the heat exchanger:

Heat-exchanger frontal area, sq ft	0.813
Air-side free-flow area, sq ft	0.386
Air-side heat-transfer area, sq ft	45.9
Fuel-side heat-transfer area, sq ft	4.6
Air-side hydraulic radius, ft	0.0049

Over-All Heat-Transfer Coefficient Needed to Vaporize All Fuel

The over-all heat-transfer coefficient necessary for complete vaporization of the fuel required by the engine was calculated from the relation between heat-exchanger effectiveness E and the maximum number of heat-transfer units NTU. This relation was obtained from reference 9 for a crossflow evaporator and is reproduced in figure 16. To use this relation the air temperature drop was calculated from a heat balance:

$$w_a c_{p,a} \Delta T_a = w_f H_L$$

The latent heat of vaporization of liquid hydrogen, obtained from reference 10, is 168 Btu/lb at 46° R.

Thus,

$$\Delta T_a = \frac{520 \times 168}{1.75 \times 3600 \times 0.24} = 57.8^\circ \text{ R} \qquad \text{(B1)}$$

and

$$E = \frac{\Delta T_a}{T_{a,2} - T_f} = \frac{57.8}{437 - 46} = 0.148 \qquad \text{(B2)}$$

Then, from figure 16,

$$NTU = \frac{A_a U_a}{w_a c_{p,a}} = 0.15$$

from which the over-all heat-transfer coefficient based on the air-side heat-transfer area was calculated:

$$U_a = \frac{0.15 \times 1.75 \times 3600 \times 0.24}{45.9} = 4.95 \text{ Btu/(hr)(sq ft)(}^\circ\text{R)}$$

Over-All Heat-Transfer Coefficient Calculated from

Expected Air- and Fuel-Side Film Coefficients

The over-all heat-transfer coefficient expected for the particular core geometry and operating conditions was calculated from the air- and fuel-side film coefficients by using the following equation:

$$\frac{1}{U_a} = \frac{1}{\eta_o h_a} + \frac{1}{\frac{A_f}{A_a} h_f} \tag{B3}$$

Although the core of this heat exchanger was not exactly like any of those included in reference 9, its air-side heat-transfer characteristic was estimated from that data and the air-side Reynolds number. The Reynolds number was calculated as follows:

$$Re = \frac{4r_h \frac{w_a}{A_c}}{\mu} = \frac{4 \times 0.0049 \times 1.75 \times 3600}{0.386 \times 0.036} = 8900 \tag{B4}$$

Where the viscosity μ of air was taken from reference 11 at the average air temperature of 408° R, the air-side heat-transfer characteristic $(h_a A_c / w_a c_{p,a})(Pr)^{2/3}$ was estimated to be 0.004 from reference 9. The air-side film coefficient was then calculated:

$$h_a = \frac{0.004 \times 1.75 \times 3600 \times 0.24}{0.386 \times 0.815} = 19.2 \text{ Btu/(hr)(sq ft)(°R)}$$

The value of Prandtl number Pr was taken from reference 11 at the average air temperature.

The over-all fin efficiency η_o is a function of the geometry of the core and the air-side film coefficient. A value of the fin efficiency for this core of 0.95 was calculated from the data in reference 9.

The fuel-side film coefficient was estimated from the hydrogen pot-boiling data of reference 7 and the average temperature difference between the tube wall and the fuel. The average wall temperature was calculated from the air-side film coefficient as follows:

$$w_f H_L = -h_a A_a \left(T_{a,2} - \frac{\Delta T_a}{2} - T_w \right) \tag{B5}$$

$$520X168 = -19.2X45.9 \left(437 - \frac{57.8}{2} - T_w\right)$$

and

$$T_w = 309^\circ \text{ R}$$

from which the temperature difference between the wall and the fuel is

$$T_w - T_f = 309 - 46 = 263^\circ \text{ R}$$

The fuel-side film coefficient was estimated to be 71.5 Btu/(hr)(sq ft)($^\circ$R). Substituting these values into equation (B3) yields

$$\frac{1}{U_a} = \frac{1}{0.95X19.2} + \frac{\frac{1}{4.6}}{45.9} 71.5 = 0.0548 + 0.139$$

and $U_a = 5.15$ Btu/(hr)(sq ft)($^\circ$R).

Comparison of the over-all heat-transfer coefficient required to vaporize all the fuel and the over-all coefficient calculated from the expected air- and fuel-side film coefficients indicated that the core selected would be slightly conservative.

Air-Side Total-Pressure Loss

The following equation was used to calculate the air-side total-pressure loss of the heat exchanger:

$$\frac{\Delta p}{p_1} = \frac{G^2}{2g} \frac{1}{\rho_1 p_1} \left\{ \left[1 + \left(\frac{A_c}{A_{fr}} \right)^2 \right] \left(\frac{\rho_1}{\rho_2} - 1 \right) + \left(f \frac{A_a}{A_c} \frac{\rho_1}{\rho_m} \right) \right\} \qquad (6)$$

A friction factor f of 0.017 was estimated from the data presented for similar heat exchangers in reference 9. Because the Mach numbers entering and leaving the heat exchanger were below 0.2, it was assumed the static and total pressures were equal. With these assumptions a total-pressure loss of 53 lb/sq ft was calculated. Since the difference between total and static pressures in flight was 110 lb/sq ft, this core was considered satisfactory.

REFERENCES

1. Silverstein, Abe, and Hall, Eldon W.: Liquid Hydrogen as a Jet Fuel for High-Altitude Aircraft. NACA RM E55C28a, 1955.

2. Lewis Laboratory Staff: Hydrogen for Turbojet and Ramjet Powered Flight. NACA RM E57D23, 1957.

3. Braithwaite, Willis M., Fenn, David B., and Algranti, Joseph S.: Altitude-Chamber Evaluation of an Aircraft Liquid-Hydrogen Fuel System Used with a Turbojet Engine. NACA RM E57F13a, 1957.

4. Otto, Edward W., Hiller, Kirby W., and Kohl, Robert C.: Design and Performance of Fuel Control for Hydrogen Aircraft Fuel System. NACA RM E57F19, 1957.

5. Corrington, Lester C., Thornbury, Kenneth L., and Hennings, Glenn: Some Design and Operational Considerations of a Liquid-Hydrogen Fuel and Heat-Sink System for Turbojet-Engine Tests. NACA RM E56J18a, 1956.

6. Straight, David M., Smith, Arthur L., and Christenson, Harold H.: Brief Studies of Turbojet Combustor and Fuel-System Operation with Hydrogen Fuel at -400° F. NACA RM E56K27a, 1956.

7. Mulford, Robert N., and Nigon, Joseph P.: Heat Exchange Between a Copper Surface and Liquid Hydrogen and Nitrogen. LA-1416, Tech. Info. Service, U.S. Atomic Energy Comm., May 21, 1952.

8. Sanders, Newell D., and Behun, Michael: Generalization of Turbojet-Engine Performance in Terms of Pumping Characteristics. NACA TN 1927, 1949.

9. Kays, W. M., and London, A. L.: Compact Heat Exchangers. The Nat. Press, Palo Alto (Calif.), 1955.

10. Woolley, Harold W., Scott, Russell B., and Brickwedde, F. G.: Compilation of Thermal Properties of Hydrogen and Its Various Isotopic and Ortho-Para Modifications. Jour. Res. Nat. Bur. Standards, vol. 41, no. 5, Nov. 1948, pp. 379-475.

11. McAdams, William H.: Heat Transmission. Third Ed., McGraw-Hill Book Co., Inc., 1954.

TABLE I. - HEAT-EXCHANGER PERFORMANCE

Run	Air-flow, $W_{a,1}$, lb/sec	Fuel flow, W_f, lb/hr	Inlet air temper-ature, $T_{a,2}$, °R	Air temper-ature drop, ΔT_a, °R	Inlet fuel temper-ature, T_f, °R	Fuel temper-ature rise, ΔT_f, °R	Inlet wall temper-ature, $T_{w,2}$, °R	Outlet wall temper-ature, $T_{w,3}$, °R	Fuel static pressure, p_f, lb/sq in. abs	Enthalpy ratio, $\Delta H_a/H_L$	Heat-transfer coeffi-cient, h_f, Btu/(hr)(sq ft)(°F)	Inlet air total pres-sure, $P_{a,2}$, lb/sq ft abs	Total-pres-sure loss, $\frac{\Delta P_a}{P_{a,2}}$
1	1.78	351	436	53	46.5	23.0	368	328	52.9	1.40	61.1	321	0.215
2	1.77	376	441	55	46.5	15.7	364	328	53.4	1.35	63.8	322	.214
3	1.76	386	442	56	46.5	16.8	362	326	53.4	1.33	63.9	322	.214
4	1.75	409	442	57	46.4	19.6	365	326	52.9	1.26	64.2	319	.213
5	1.75	412	442	57	47.4	19.6	365	326	54.3	1.28	64.6	328	.241
6	1.75	417	442	58	46.5	14.0	364	324	52.2	1.27	65.6	320	.218
7	1.78	442	442	56	46.5	7.3	370	329	53.4	1.17	62.3	320	.209
8	1.76	451	443	59	47.4	11.6	365	324	54.3	1.22	66.5	327	.239
9	1.79	505	443	60	46.0	4.7	362	319	50.7	1.06	68.3	320	.216
10	1.83	151	434	41	46.6	90.4	396	357	55.4	2.59	49.6	390	.133
11	1.80	322	437	53	46.8	28.2	368	328	55.4	1.55	62.4	323	.214
12	1.82	372	439	55	46.7	21.9	367	328	54.4	1.40	64.7	319	.219
13	1.84	387	435	54	46.5	19.0	362	323	53.4	1.33	64.6	321	.231
14	1.87	387	440	53	46.3	10.4	369	331	52.4	1.32	62.1	330	.227
15	1.80	396	441	54	46.3	10.4	370	332	52.4	1.27	60.9	324	.216
16	1.80	436	444	57	46.0	18.2	366	328	51.4	1.19	66.3	323	.211
17	1.84	451	441	57	46.5	17.3	368	323	51.4	1.22	68.0	320	.213
18	1.83	471	443	56	46.3	3.9	370	328	52.4	1.13	63.9	324	.222
19	1.86	518	440	59	46.6	3.6	360	318	53.4	1.10	70.6	323	.223
20	2.02	265	430	41	46.6	52.4	384	346	56.9	1.63	53.3	383	.181
21	2.10	325	431	45	46.6	33.4	378	341	55.9	1.51	59.6	394	.179
22	2.11	354	439	47	46.9	29.7	386	345	55.4	1.47	61.2	391	.192
23	2.11	400	439	48	47.0	22.5	384	341	53.4	1.33	62.2	390	.192
24	2.12	459	432	50	46.3	9.2	370	327	53.9	1.19	66.7	387	.202
25	2.12	457	435	50	46.6	10.7	377	334	52.9	1.21	65.4	389	.203
26	2.07	471	438	49	46.2	1.0	381	338	51.9	1.11	60.6	386	.187
27	2.16	480	438	49	46.7	7.3	377	333	52.9	1.15	65.0	391	.205
28	2.15	499	435	51	46.5	5.7	373	327	54.9	1.14	68.3	397	.204
29	2.13	527	442	53	46.8	8.7	382	333	53.4	1.12	69.1	391	.192
30	2.13	567	442	53	46.2	8.6	381	330	52.4	1.03	69.5	390	.201
31	2.14	592	441	54	46.8	2.0	377	327	54.4	1.03	71.6	387	.222
32	2.17	608	442	51	45.8	1.4	382	337	52.2	.931	66.3	395	.210
33	2.17	622	437	50	45.8	1.1	377	332	51.9	.890	65.9	395	.207
34	.3607	519	451	144	45.3	----	280	216	48.2	.501	48.0	353	.017
35	.915	525	449	96	45.3	----	325	277	48.2	.838	64.4	348	.058
36	1.18	525	446	82	45.2	----	339	295	48.1	.927	66.8	350	.089
37	1.38	523	446	76	45.2	----	345	302	48.1	1.005	70.4	342	.105
38	1.61	524	448	66	45.2	----	358	314	47.8	1.014	68.4	343	.152
39	1.76	519	447	62	45.3	----	366	322	48.1	1.051	68.5	336	.211
40	1.87	523	449	59	45.3	----	388	328	48.1	1.056	66.2	333	.249
41	.537	571	449	131	47.6	.9	317	234	54.15	.639	58.1	256	.035
42	.666	578	---	---	47.5	1.4	---	---	53.7	-----	-----	269	.086
43	1.54	568	445	67	47.5	2.8	364	318	53.2	.946	65.1	308	.195
44	1.84	578	447	61	47.5	3.1	367	330	53.2	.994	70.1	329	.240
45	2.21	561	444	51	47.5	4.3	373	342	52.7	1.03	68.7	347	.354
46	.495	612	451	117	47.6	.4	309	235	53.9	.490	48.5	259	.039
47	.956	613	450	99	46.2	1.2	336	283	51.0	.798	67.5	271	.096
48	1.39	603	448	75	46.9	1.3	355	311	51.3	.905	68.3	297	.165
49	1.82	622	443	59	46.8	1.9	365	320	52.8	.904	68.3	326	.242
50	1.83	616	445	60	46.7	2.1	366	322	52.8	.927	69.3	329	.231

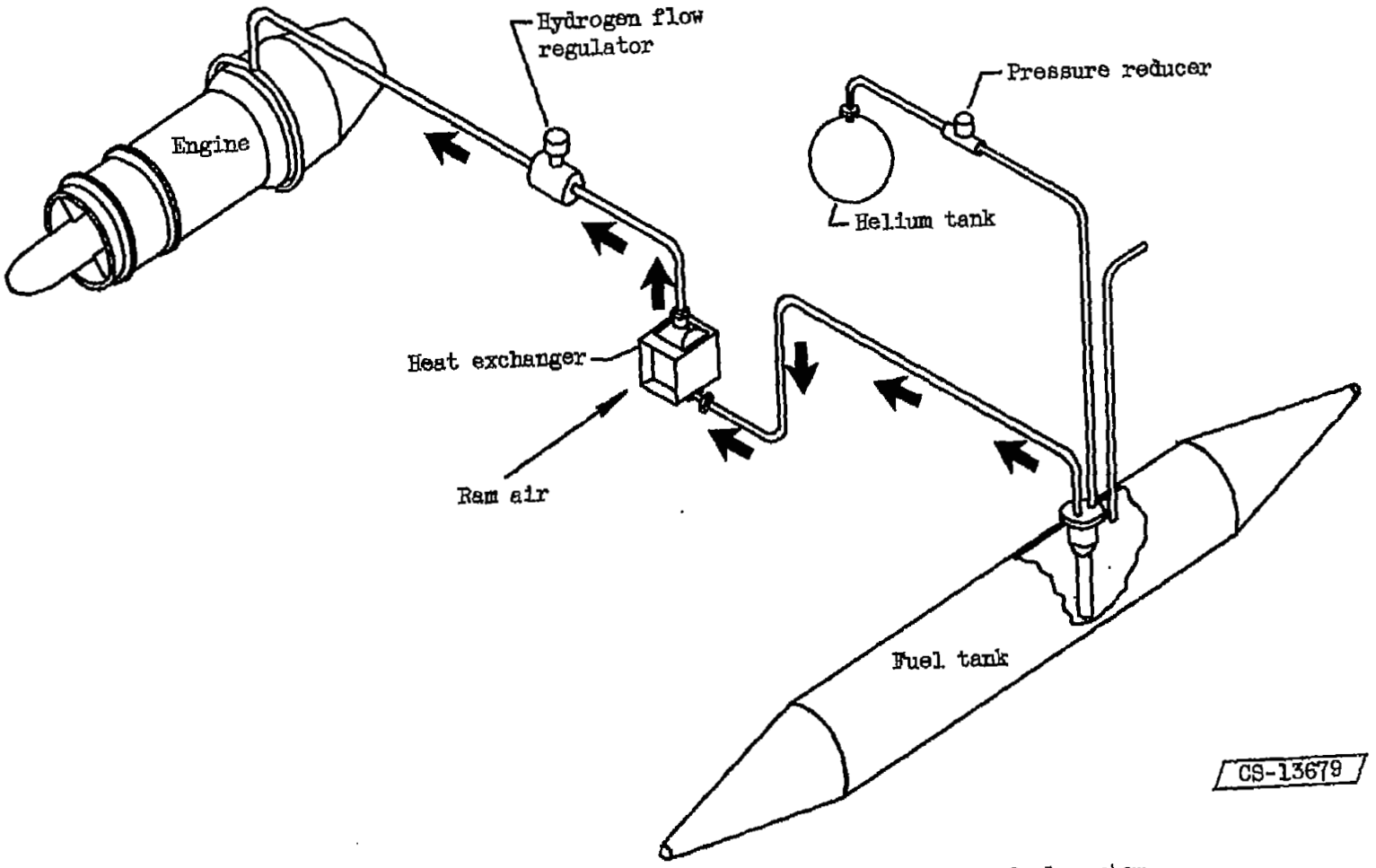

Figure 1. - Schematic diagram of aircraft liquid-hydrogen fuel system.

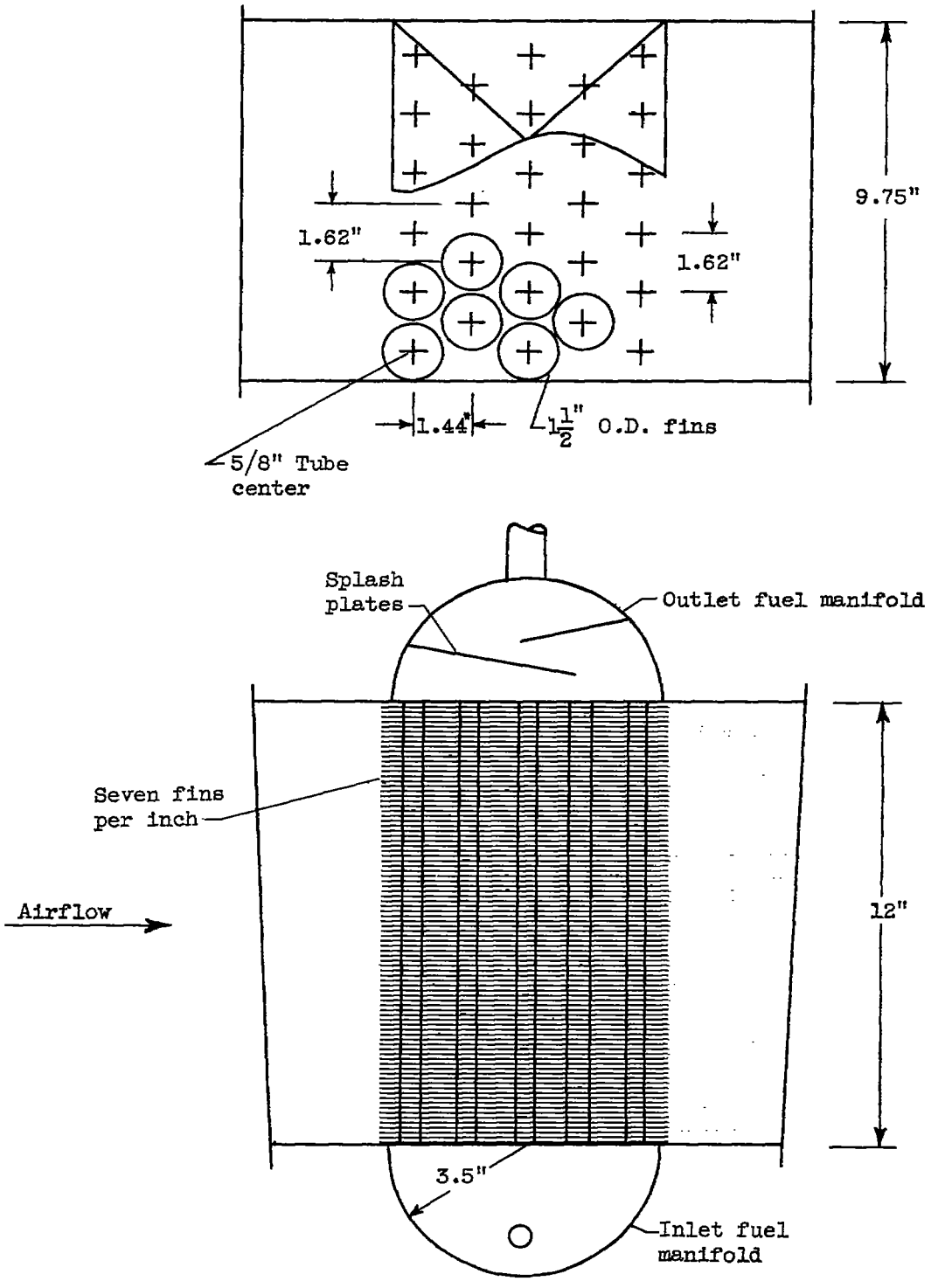

Figure 2. - Schematic diagram of heat exchanger.

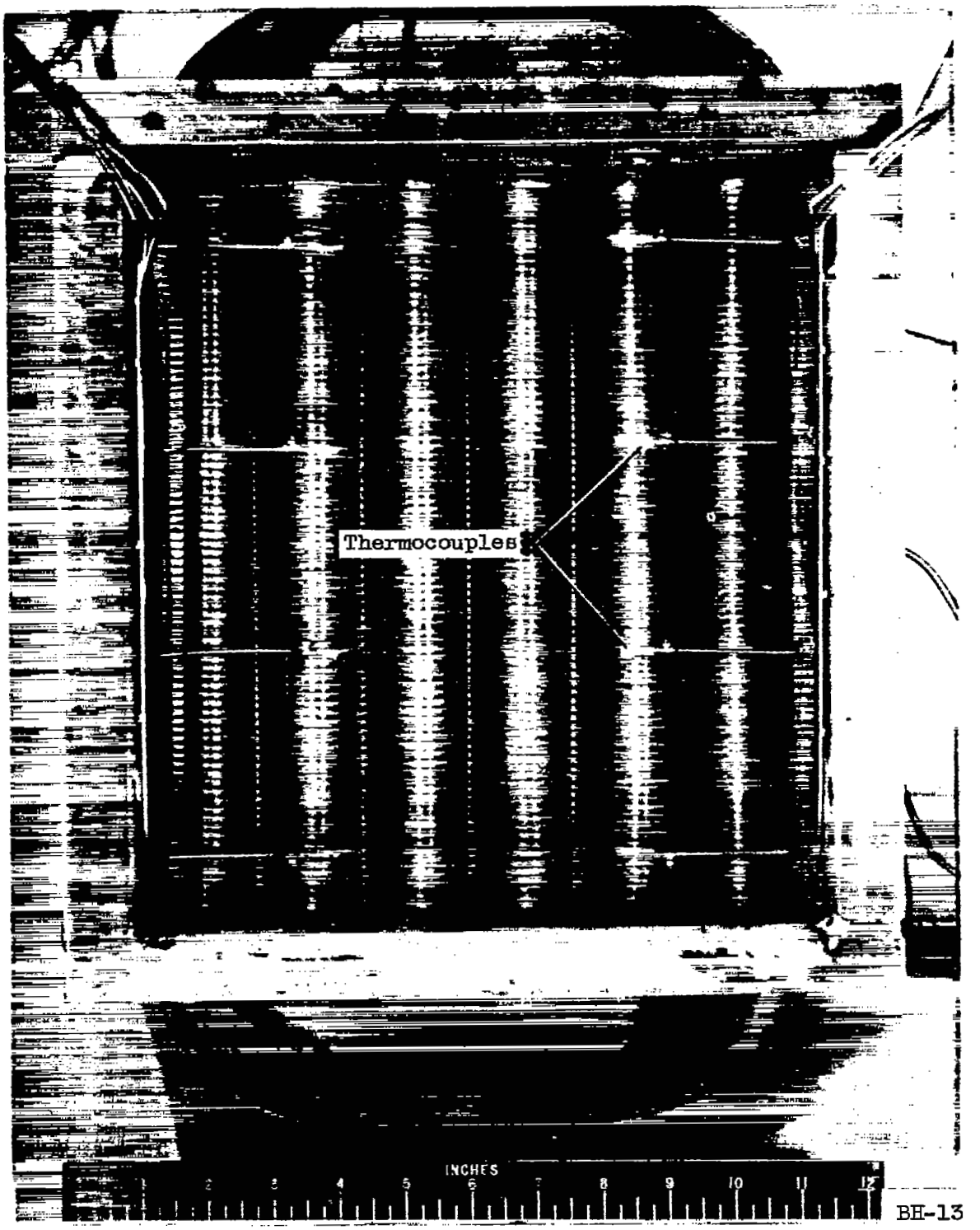

Figure 3. - Inlet air side of heat exchanger.

Figure 4. - Fuel system and engine installation in altitude test chamber.

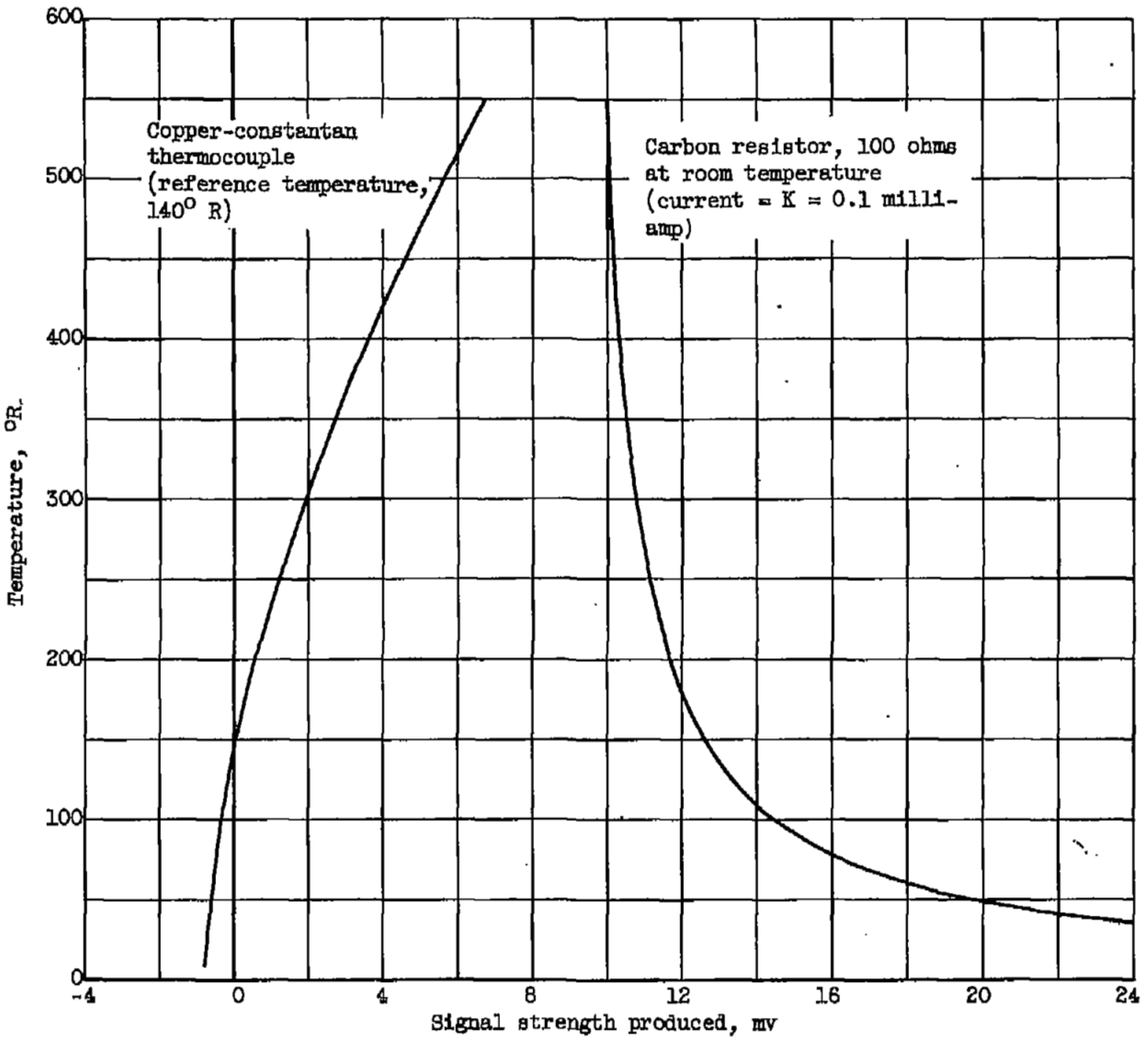

Figure 5. - Comparison of low-temperature measuring devices.

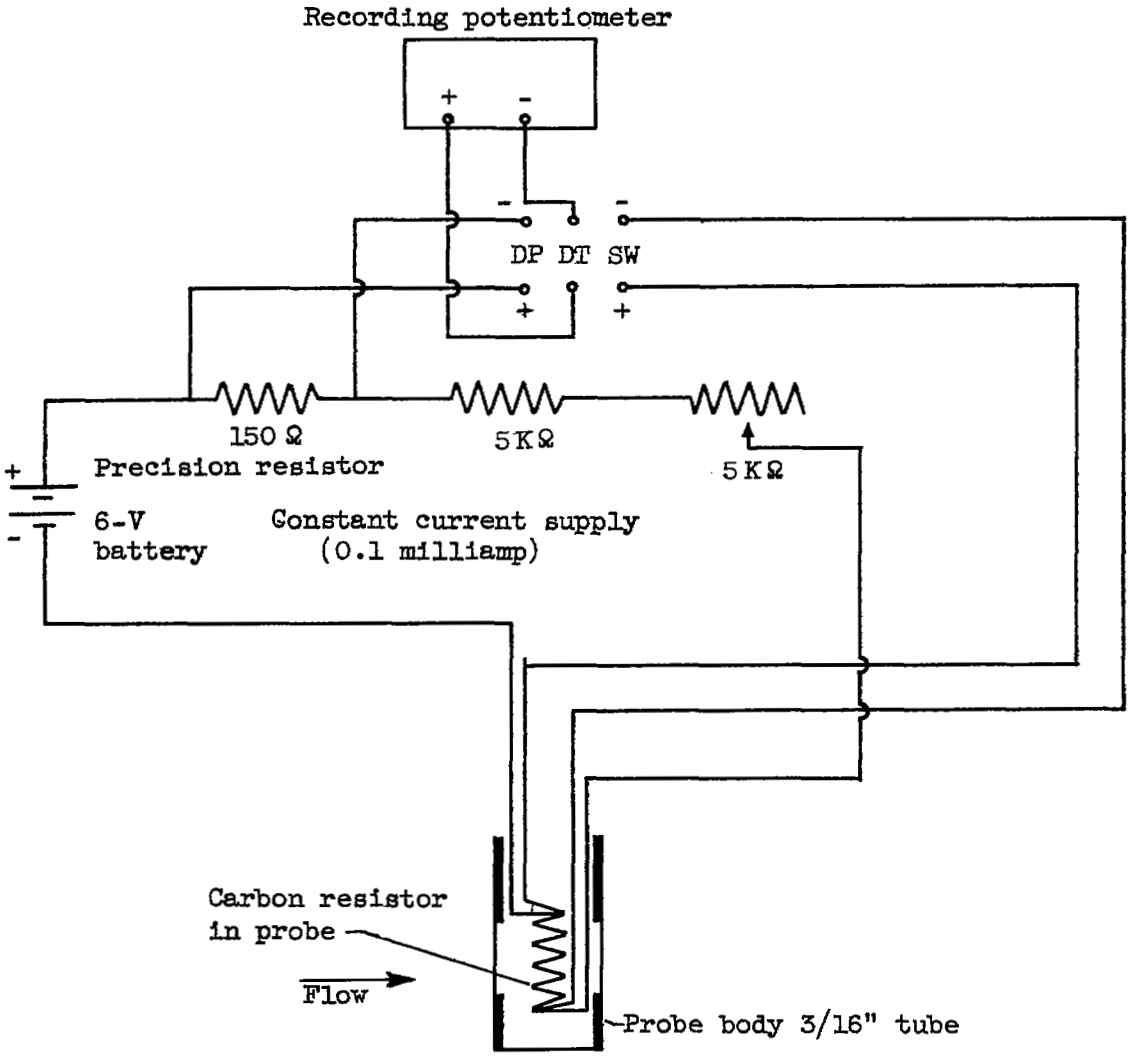

Figure 6. - Circuit diagram for carbon resistor probe.

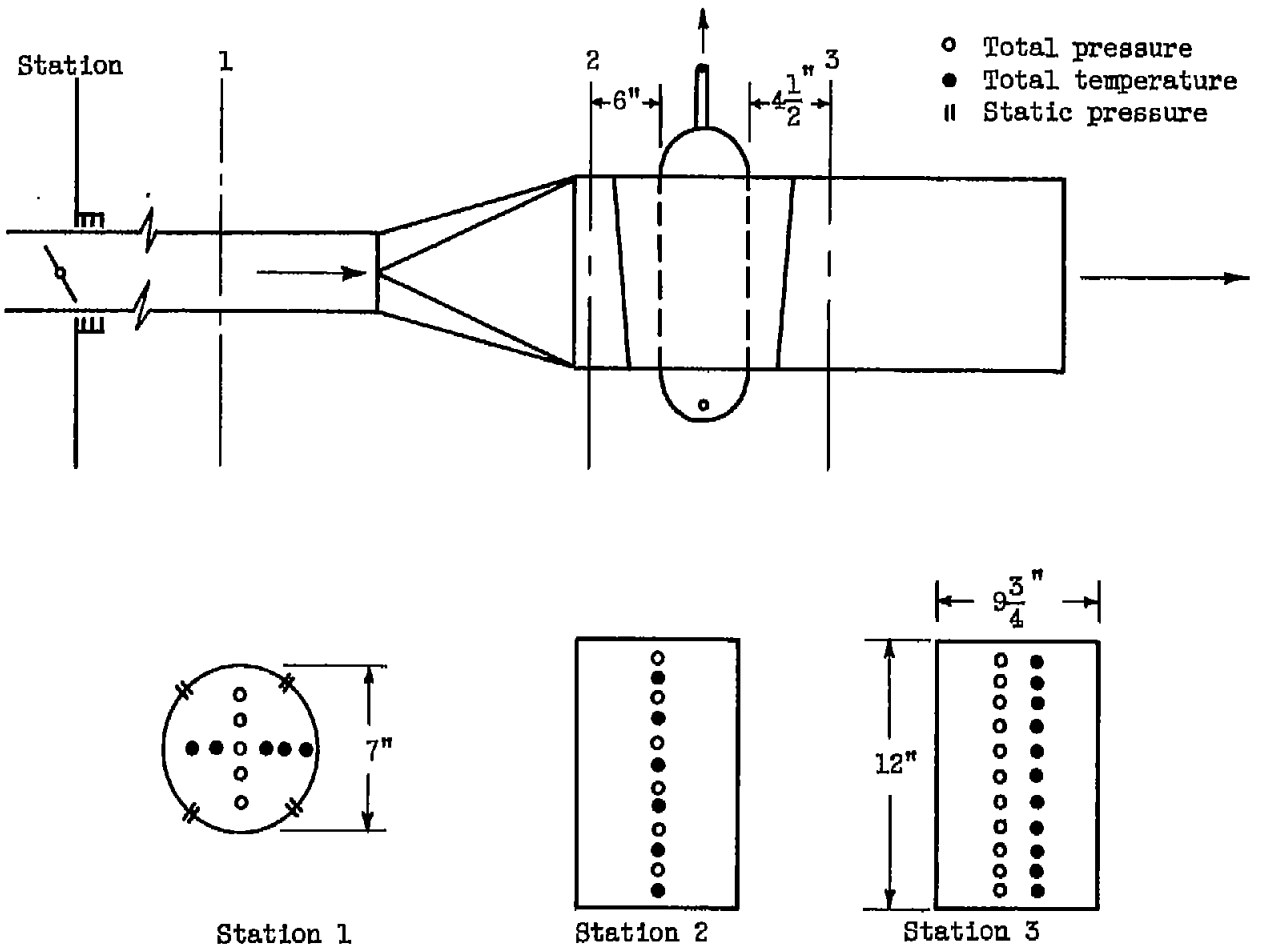

Figure 7. - Location of heat-exchanger instrumentation.

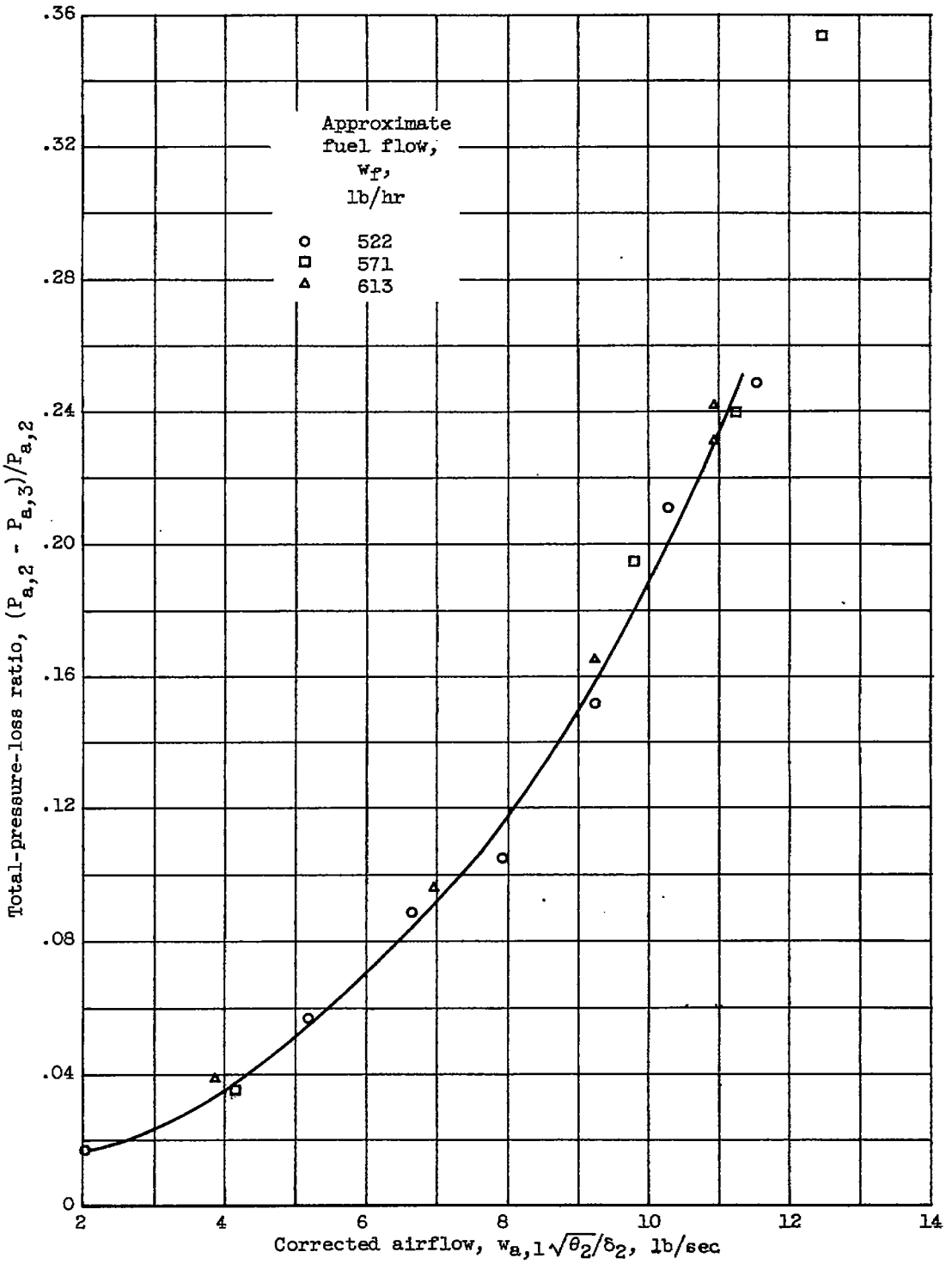

Figure 8. - Air-side total-pressure loss.

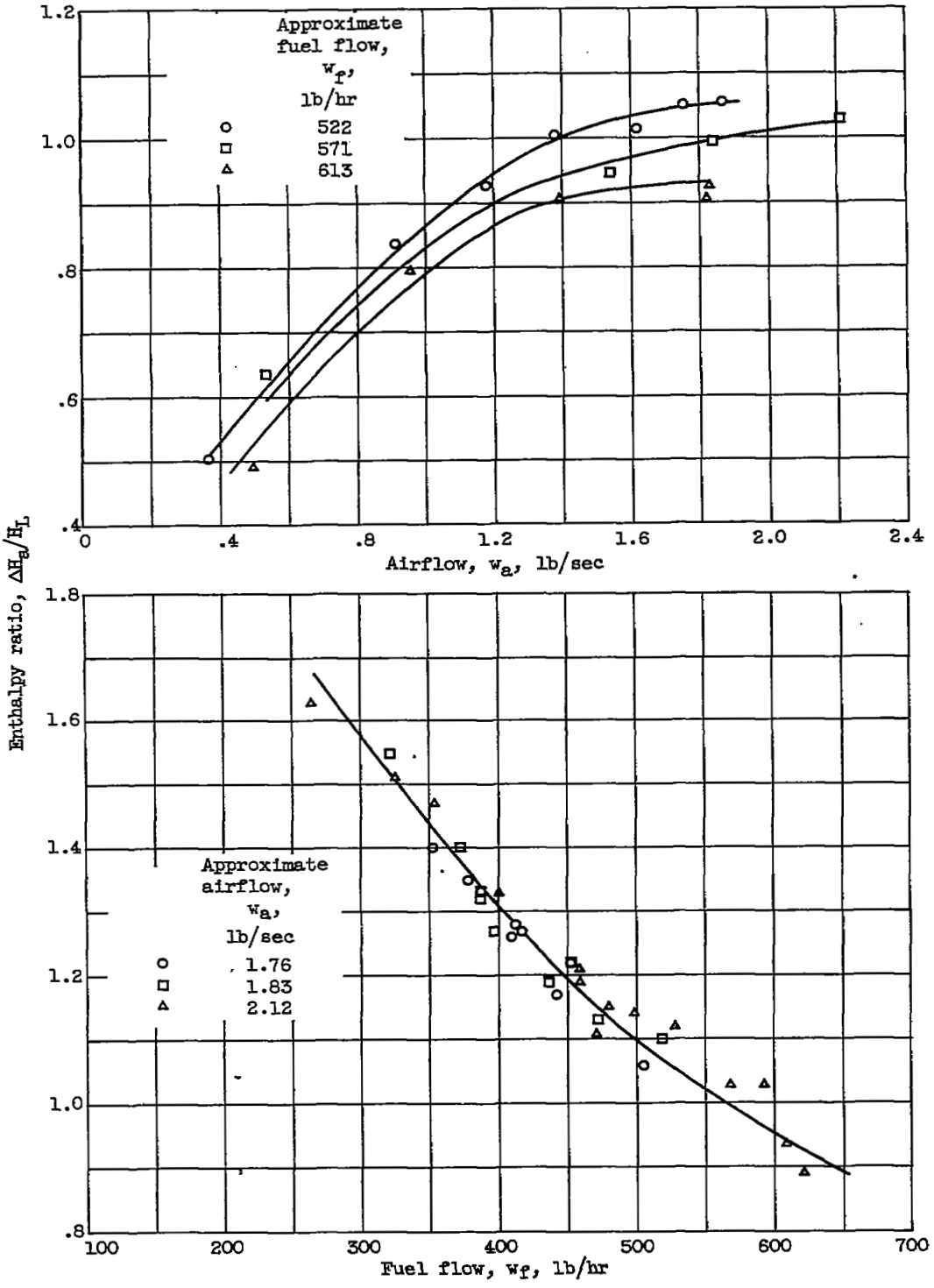

Figure 9. - Ratio of heat lost by air to latent heat of vaporization of fuel.

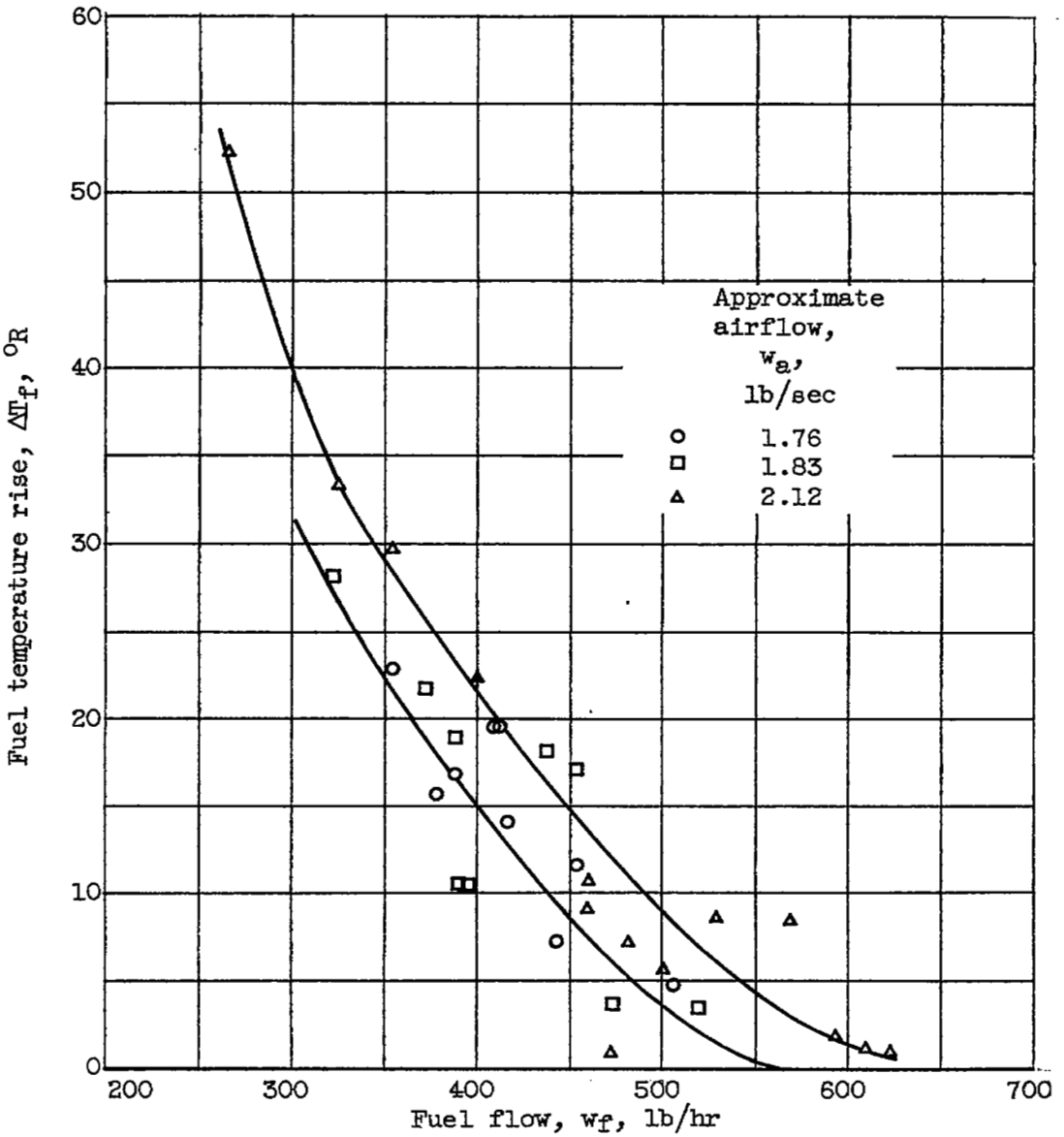

Figure 10. - Fuel temperature rise.

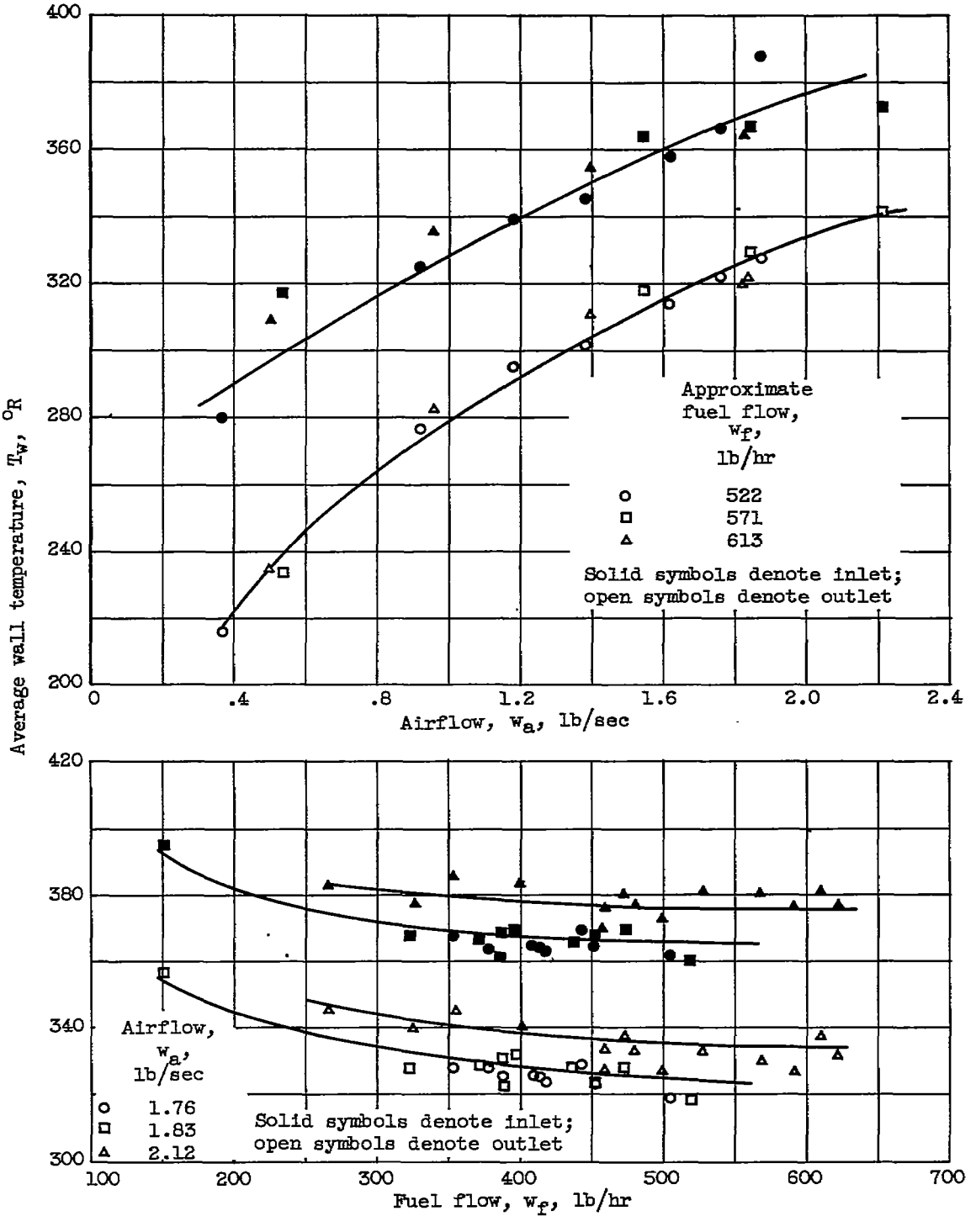

Figure 11. - Average wall temperature for air inlet and outlet banks of tubes.

[redacted]

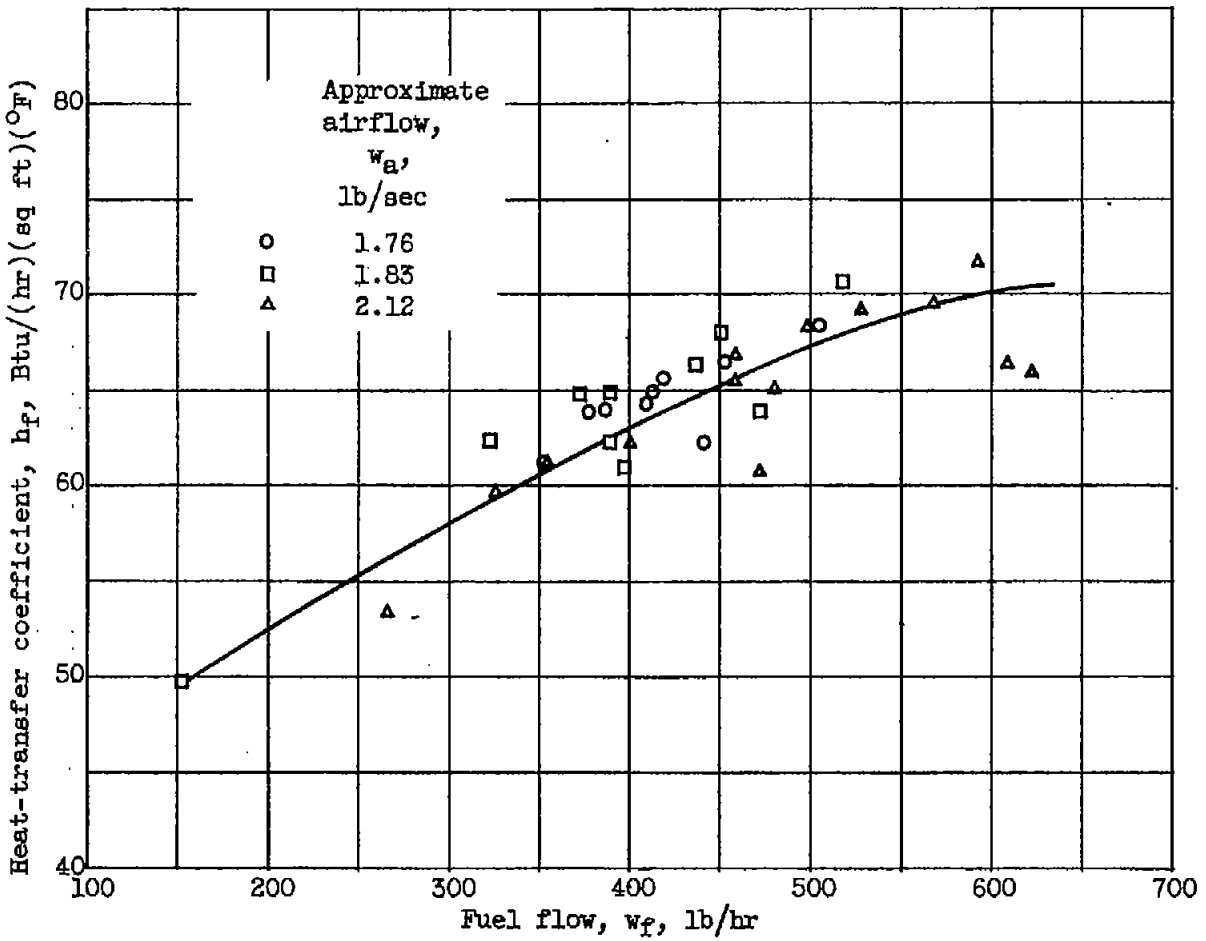

Figure 12. - Fuel-side film coefficient.

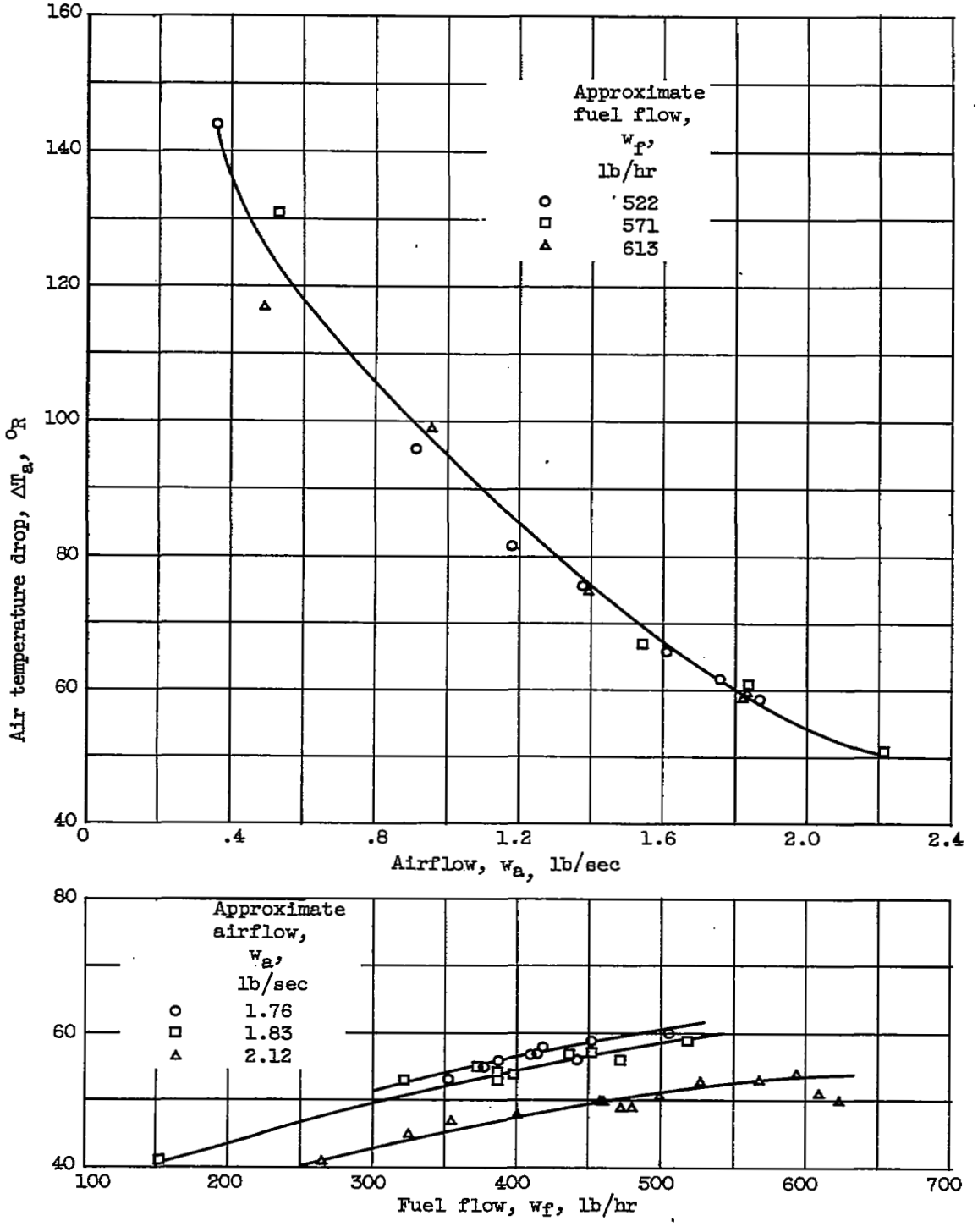

Figure 13. - Air-side temperature drop.

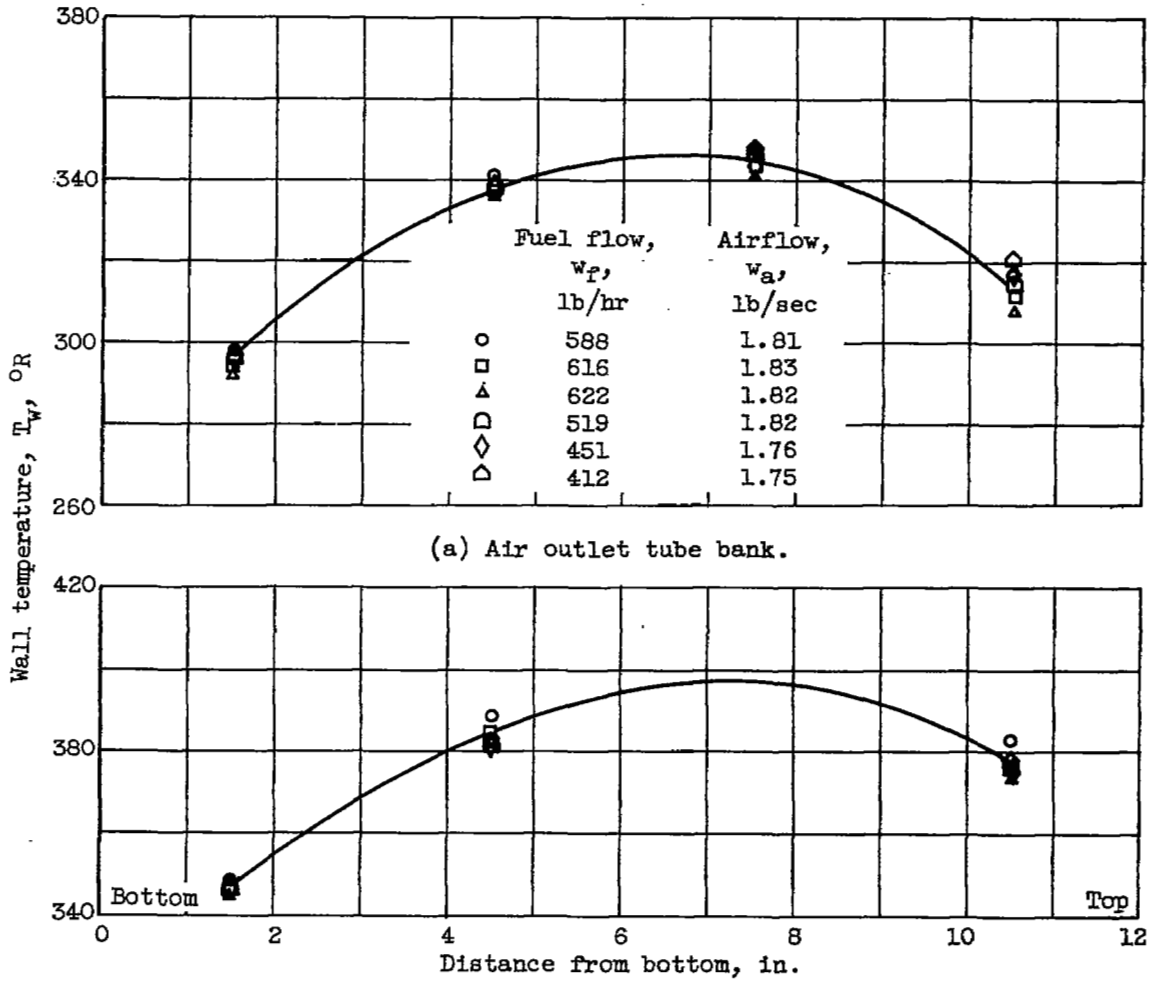

(a) Air outlet tube bank.

(b) Air inlet tube bank.

Figure 14. - Wall temperature gradients for air inlet and outlet banks of tubes.

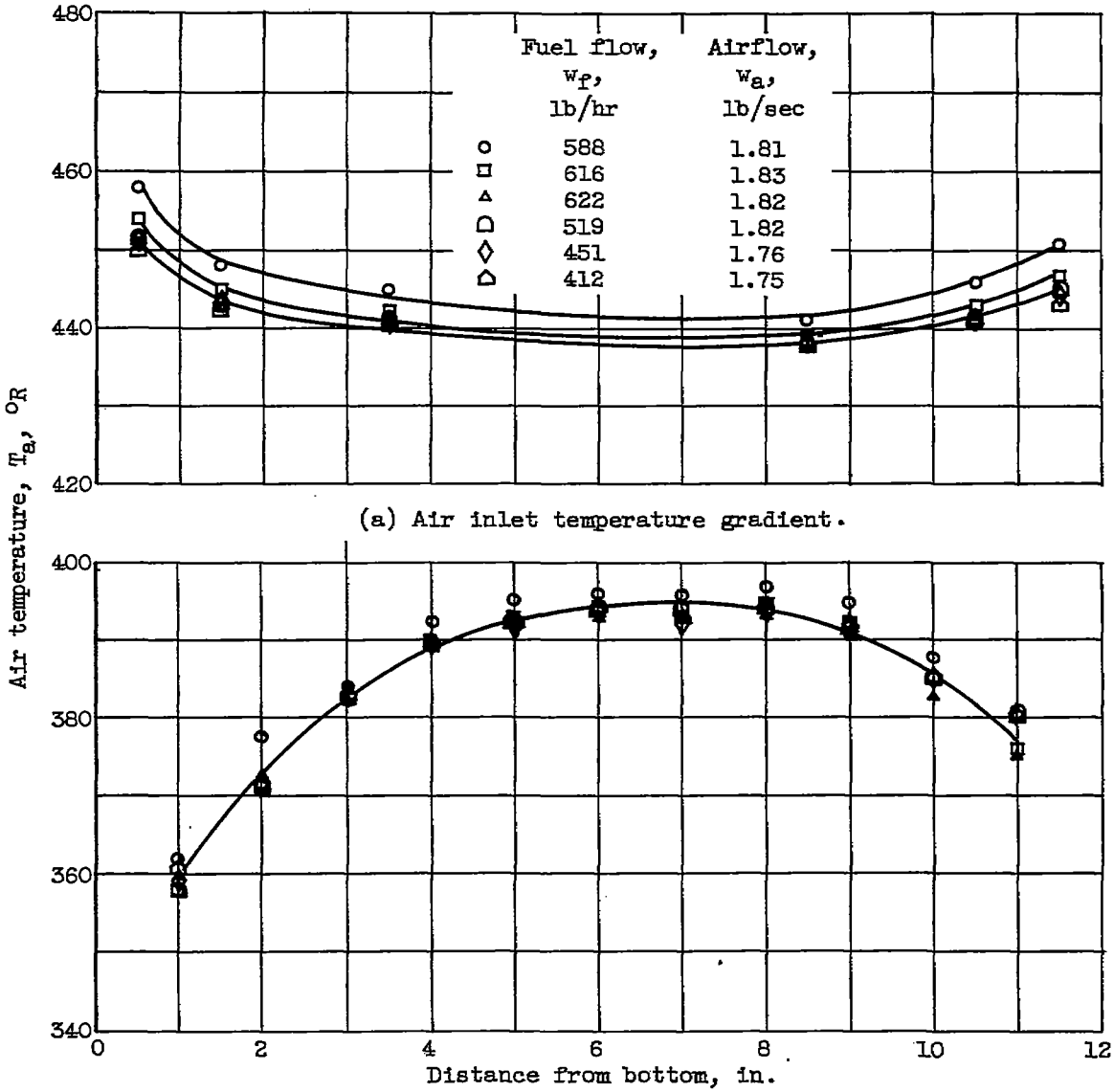

(a) Air inlet temperature gradient.

(b) Air outlet temperature gradient.

Figure 15. - Air temperature at inlet and outlet of heat exchanger.

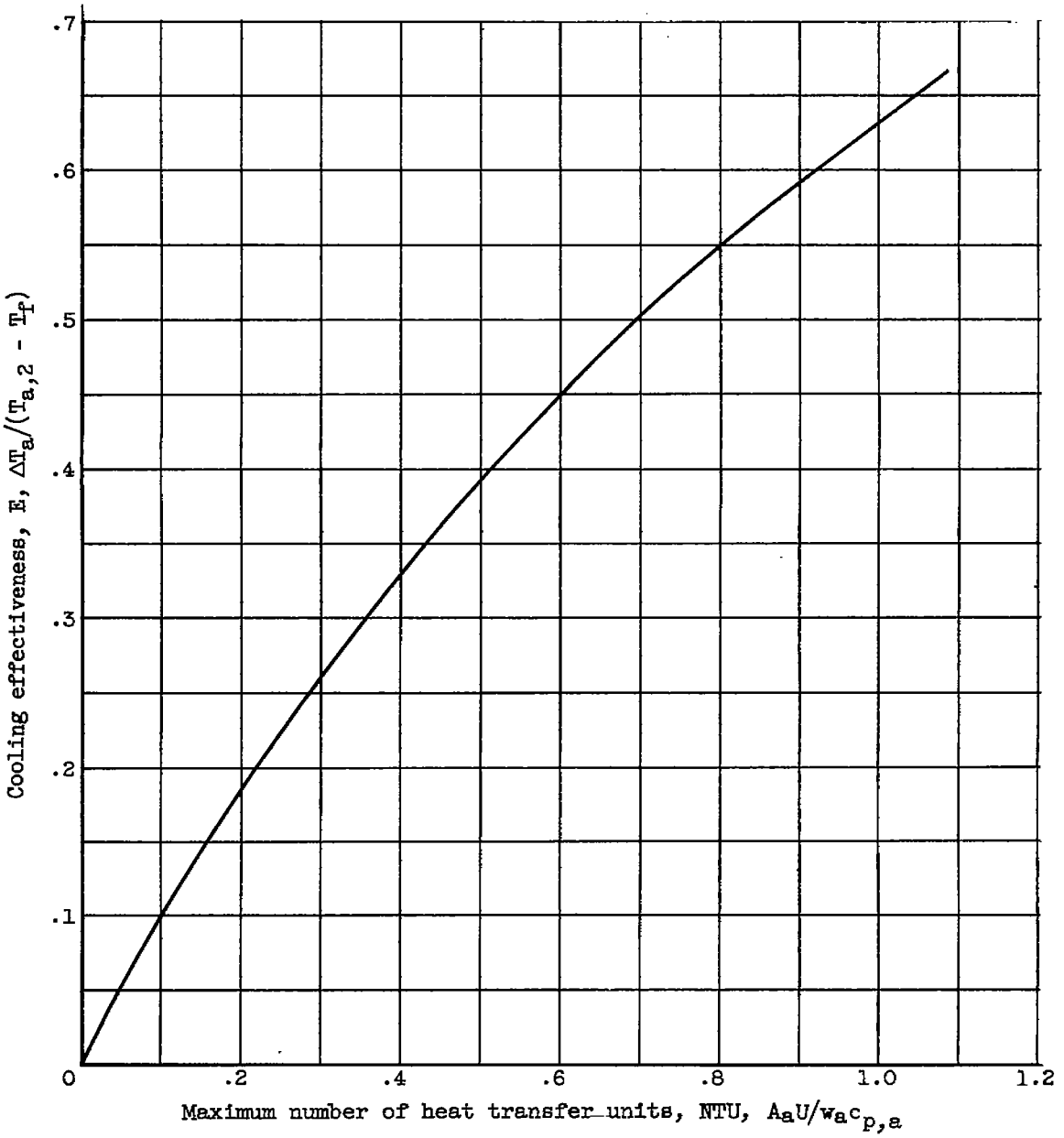

Figure 16. - Relation of cooling effectiveness to quantity NTU for crossflow evaporator (ref. 9).